

Article

# Numerical Simulation Study of Winter Pollutant Transport Characteristics over Lanzhou City, Northwest China

Jianjun He <sup>1,\*</sup>, Shuhua Lu <sup>1</sup>, Ye Yu <sup>2</sup>, Sunling Gong <sup>1</sup>, Suping Zhao <sup>2</sup> and Chunhong Zhou <sup>1</sup>

<sup>1</sup> State Key Laboratory of Severe Weather & Key Laboratory of Atmospheric Chemistry of CMA, Chinese Academy of Meteorological Sciences, Beijing 100081, China; lushuhua526@163.com (S.L.); gongsl@cma.gov.cn (S.G.); zhouch@cma.gov.cn (C.Z.)

<sup>2</sup> Northwest Institute of Eco-Environment and Resources, Chinese Academy of Sciences, Lanzhou 730000, China; yyu@lzb.ac.cn (Y.Y.); zhaosp@lzb.ac.cn (S.Z.)

\* Correspondence: hejianjun@cma.gov.cn; Tel.: +86-010-5899-4164

Received: 7 September 2018; Accepted: 28 September 2018; Published: 1 October 2018



**Abstract:** Air pollution levels are severe in Lanzhou due to the valley topography and the semi-arid climate. A comprehensive understanding of pollutant transport characteristics, which are affected by atmospheric circulation, can help explain the reason for the air pollution to some extent. Using the Weather Research and Forecast (WRF) model coupled with the FLEXible PARTicle (FLEXPART) dispersion model, the authors of this paper simulated the transport pathways of pollutants discharged from local sources and analyzed the diffusion efficiency over Lanzhou during six winters from 2002 to 2007. Flow field analysis showed that a divergence and convergence region formed in the Lanzhou valley during the day and at night, respectively. The Lanzhou valley was dominated by an easterly wind. Based on transport trajectories from FLEXPART, five main transport pathways, namely, the southwest pathway (SW), west pathway (W), south pathway (S), southeast pathway (SE), and northeast pathway (NE), were identified over Lanzhou. Compared with static weather, it was easier for pollutants to cross the south mountain (i.e., along the southeast pathway) during the strong cold air process. The percentage of particles moving out of the urban valley after 12 h of transport and the ratio of particles moving back into the urban valley showed significant diurnal variability. This indicates that the air pollution over Lanzhou may be reduced to some extent by artificially controlling the emission time of pollutants.

**Keywords:** WRF; FLEXPART; transport trajectory; local circulation

## 1. Introduction

With the changes in global climate and the rapid urbanization process, urban air pollution in developing countries has become a hot issue in the world. As the largest developing country, China is suffering from serious air pollution. The annual average PM<sub>2.5</sub> concentration for major Chinese cities in 2014 exceeded 82% of the Chinese Ambient Air Quality Standards (CAAQS) Grade II standard (35  $\mu\text{g m}^{-3}$ ) and was 6.4 times the guideline value recommended by the World Health Organization (WHO) [1]. Serious air pollution results in high health risks for people in China [2]. O<sub>3</sub> pollution also affects ecosystems and agriculture [3]. Pollution levels are affected by multiple factors such as pollutant emissions, meteorological conditions, topography, dry and wet deposition, and secondary pollutants generated by photochemical reactions [4–7]. China is the largest pollutant emitter in the world [8]. The large amount of pollutant emissions, especially industrial and transportation emissions, is the root cause of the serious air pollution in China. According to the China Statistical Yearbook, sulfur dioxide, nitric oxide, and dust emissions were  $1.1 \times 10^7$ ,  $1.39 \times 10^7$ , and  $1.01 \times 10^7$  ton, respectively,

in 2016 [9]. Meteorological conditions are important factors that influence pollution levels and explain more than 70% of the variance in pollutant concentrations [1]. Adverse meteorological conditions can easily produce serious air pollution [10].

Lanzhou is located at the junction of the western end of the Loess Plateau and the northeastern part of the Qinghai-Tibet Plateau. With an average elevation of 1520 m, urban Lanzhou is located in the Yellow River Gorge. The surrounding mountain height ranges from 200 to 600 m [11]. Lanzhou valley is a continental arid and semi-arid region with an annual average 2-m temperature of 9.3 °C and an annual average 10-m wind speed of 0.8 m s<sup>-1</sup>. The annual total precipitation is 327.7 mm, of which 50% falls during July–October [12]. In the 1950s, a number of key industrial projects began to settle in Lanzhou. Numerous emission sources, valley topography, and adverse meteorology have resulted in serious air pollution in Lanzhou [13]. Meteorological conditions, especially local meteorological conditions, are the main factors that determine the day-to-day variation of pollutant concentrations in Lanzhou [14]. Based on observations, the daytime inversion caused by the mountain heating effect is a key factor in controlling air pollution [15]. Numerical simulations have revealed that the limited atmospheric environmental capacity, which describes the maximum potential ability of the atmosphere to purify air pollutants, has resulted in air pollution [16]. Reforestation can strengthen the mountain–valley wind and decrease air pollution in Lanzhou [17]. Using the Hybrid Single-Particle Lagrangian Integrated Trajectory (HYSPLIT) model, potential source areas in urban Lanzhou have been identified [18].

Although many previous studies have investigated the characteristics and causes of air pollution in Lanzhou, the pollutant transport characteristics and pathways from local emission sources to outside of the valley are still unclear. Based on a numerical simulation using the Weather Research and Forecast (WRF) model coupled with the FLEXible PARTicle (FLEXPART) dispersion model, the authors of this paper analyzed the transport pathways of pollutants discharged from local sources and the diffusion efficiency in Lanzhou in winter.

## 2. Numerical Simulation

### 2.1. WRF Model

WRF is a new-generation high-resolution mesoscale forecasting and data assimilation system developed jointly by the National Center for Atmospheric Research (NCAR) and the National Oceanic and Atmospheric Administration (NOAA). It includes two dynamical cores: the Advanced Research WRF (ARW) and the Nonhydrostatic Mesoscale Model (NMM). It can be used for simulation studies with a spatial resolution from 10<sup>1</sup> to 10<sup>6</sup> m, including idealized simulations (e.g., large-eddy, baroclinic wave, and mountain flow simulations) and parameterization research, data assimilation research, forecast research, etc. [19]. WRF-ARW V3.3 was used in this study.

WRF was configured as four nested domains with a resolution of 27 km, 9 km, 3 km, and 1 km (Figure 1a). Urban Lanzhou is located in the center of domain four. The terrain surrounding Lanzhou is shown in Figure 1b. In the vertical level, the atmosphere was divided into 35 levels, with 16 levels under 2 km. The pressure at the top level was 50 hPa. Initial and boundary conditions were provided by the 6 h Final (FNL) Operational Global Analysis data by the National Centers for Environmental Prediction (NCEP) at 1° × 1° horizontal resolution. The simulation periods covered six winters (Dec. to Feb.) from 2002 to 2007. The meteorological field was simulated once per month with 24 h of spin-up time. Analysis nudging was used to ensure that the upper-air model predictions did not drift too far away from the analysis data. The physical parameterization schemes included the Single-Moment 6-class microphysics scheme [20], the Kain–Fritsch cumulus parameterization scheme [21], the Rapid Radiative Transfer Model longwave [22], the Dudhia shortwave radiation parameterization scheme [23], the Yonsei University planetary boundary layer parameterization scheme [24], and the Noah land surface model (LSM) parameterization scheme [25]. These parameterization schemes have been sufficiently evaluated in previous studies [14,17,26,27].

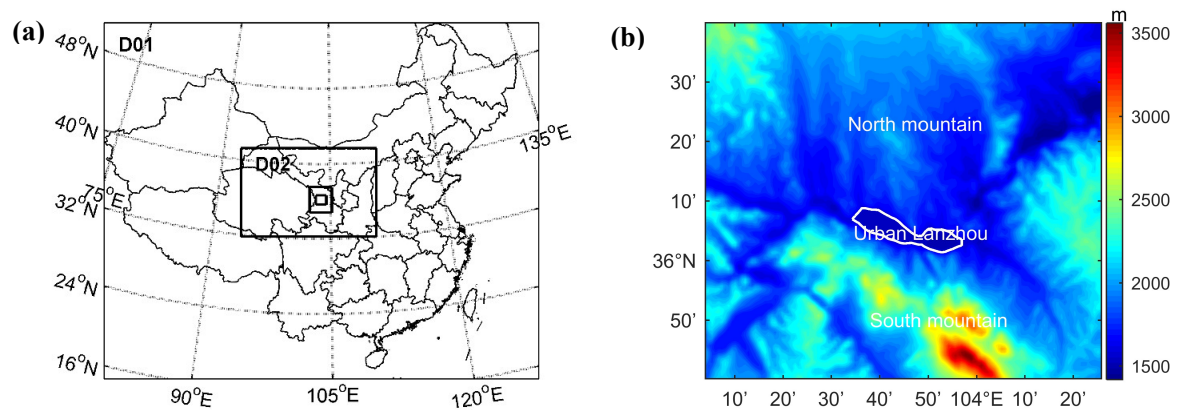


**Figure 1.** (a) Domain setting of the Weather Research and Forecast (WRF), and (b) the terrain for domain 4 and the location of Lanzhou.

## 2.2. FLEXPART Model

FLEXPART is an offline Lagrangian transport and dispersion model developed by the Norwegian Institute for Air Research (NILU). This model avoids numerical diffusion and can reach infinitesimal precision. It has been widely used in the research of large-scale and mesoscale transport, dry and wet deposition, radiation attenuation, and source apportionment. The WRF-FLEXPART coupling model, jointly developed by NOAA, NILU, and University of Colorado Cooperative Institute for Research in Environmental Sciences (CIRES), is suited for mesoscale and microscale transport and diffusion research [28].

The meteorological fields from domain 4 were used to drive FLEXPART. The smaller the WRF output interval was, the better the simulation generated by WRF-FLEXPART. However, reducing the WRF output interval would increase the amount of data. Previous research has shown that a one-hour interval of WRF output in complex terrain areas is enough to simulate the transport and diffusion processes by FLEXPART [29]. Therefore, the WRF output interval selected for this paper was one hour. The time step of FLEXPART was 180 s, and the output interval of FLEXPART was one hour. With high-resolution meteorology, the sub-grid terrain and convection parameterization schemes were not considered for FLEXPART.

## 3. Results

The performance of the WRF simulation is critically important for the simulation of particle trajectories. The authors have sufficiently evaluated the performance of the WRF simulation over Lanzhou with the same model settings as in a previous study [14]. Five statistical indices, including the index of agreement, the correlation coefficient, the root mean square error, the mean bias, and the mean error, were calculated. The performance was good and comparable with other research [14]; therefore, the evaluation is not presented again in this paper.

Local circulation significantly affects transport characteristics. Figure 2 shows the average 2-m temperature and 10-m wind flow field during six winters over Lanzhou. Terrain is the main influencing factor determining the near-surface temperature over Lanzhou: the lower the terrain is, the higher the temperature. Land cover is another important factor influencing near-surface temperature. An urban heat island effect was observed, as expected, due to the difference in land cover. Affected by the mountains, significant mountain–valley wind circulations were detected over Lanzhou, with a divergence and a convergence in the valley during the day and at night, respectively. The urban heat island effect suppressed the valley wind circulation during the day, whereas it enhanced the mountain wind circulation at night. The dominant wind in the Lanzhou valley was an easterly wind.

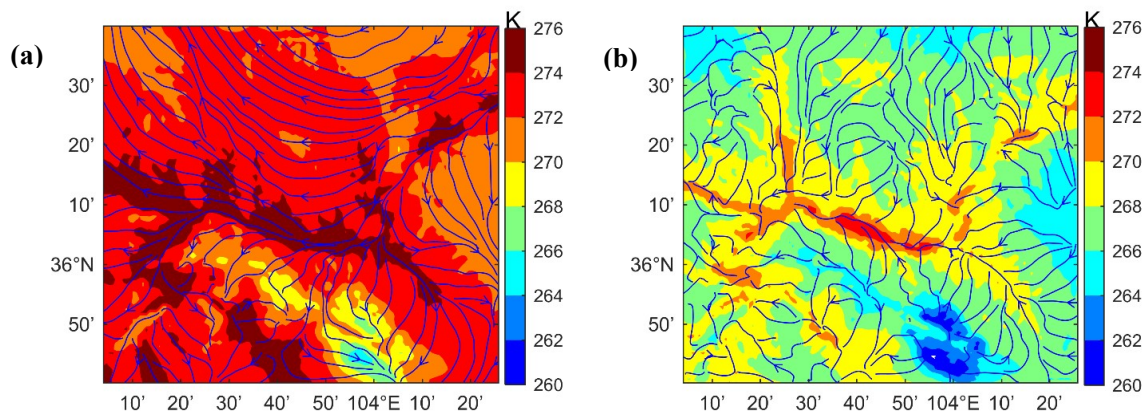


**Figure 2.** Average 2-m temperature (shading) and 10-m wind flow field (blue line) at (a) 14:00 Beijing Time (BT) and (b) 20:00 BT over Lanzhou during six winters from 2002 to 2007.

Figure 3 shows the transport trajectories of particles emitted in the east and west valleys at 14:00 Beijing Time (BT) and 20:00 BT during six winters from 2002 to 2007. The particles were released 2 m above the ground level and in the east and west valleys. Local circulation was the main factor controlling the transport of pollutants from the Lanzhou valley to the outside of the valley. Easterly winds dominated the Lanzhou valley during the day (Figure 2). Affected by the dominant wind field, most particles were transported from east to west. When the particles arrived at 103°20' E, some particles were transported south along the valley, whereas others continued to travel west until they left the research area. Because of the high terrain of the southern mountain, very few particles released from the west valley could directly pass through the southern mountain, and a small number of particles emitted in the east valley were transported outside along the western part of the southern mountain. The motion trajectory of the particles released at night was slightly different from that of particles released during the day. The proportion of the particles that travelled along the southeast valley to outside of the valley at night was higher than that during the day. In general, five typical transport channels were detected, namely, the southwest pathway (SW), west pathway (W), south pathway (S), southeast pathway (SE), and northeast pathway (NE) (Figure 4).

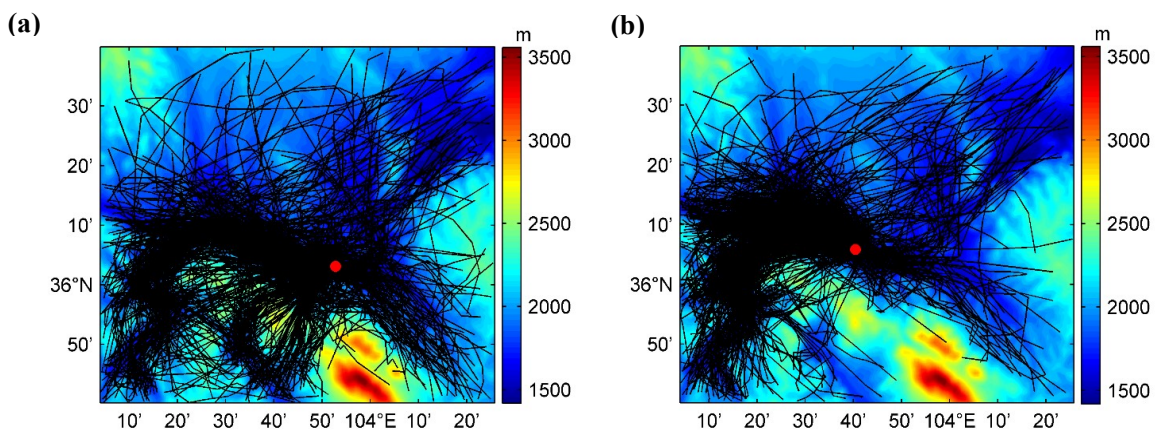


**Figure 3.** Cont.

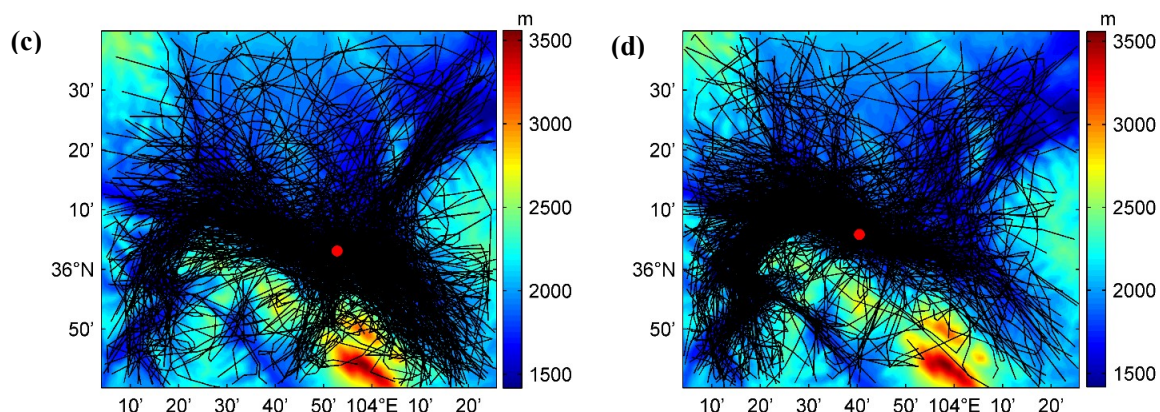


**Figure 3.** The transport trajectories of particles emitted in the east and west valleys at (a,b) 14:00 BT and (c,d) 20:00 BT during six winters from 2002 to 2007. The red points represent the emission location, emitted at 2 m above ground level. The shading represents the terrain.

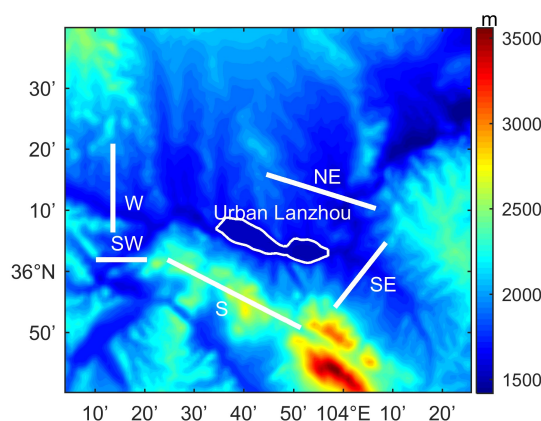


**Figure 4.** Schematic of the cross-sections of the main transport channels. The shading represents the terrain.

The authors define the percentage of particles passing through one transport channel ( $P$ ), which is calculated by Equation (1):

$$P = \frac{n}{N \times L} \times 100\% \tag{1}$$

where  $n$  is the number of particles passing through one transport channel,  $N$  is the total number of particles, and  $L$  is the length of one transport channel. The unit of  $P$  is %/km.

The synoptic-scale weather type has a significant impact on local circulation. Based on T-mode principal component analysis (PCA) combined with the K-means clustering method, eight circulation types were identified over Lanzhou during the six winters from 2002 to 2007 [14]. The strong cold air process (CT5 and CT8), weak cold air process (CT1 and CT4), stable weather (CT2, CT3, and CT7), and warm and wet air mass (CT6) were clearly identified. These data on the circulation types were used again in this paper. Table 1 shows the percentage of particles passing through the five typical transport channels under different circulation types and average states. There is a large difference between the pathways of particles released in the east and west valleys. The largest  $P$  for the east valley release is SE, followed by SW, S, NE, and W. The largest  $P$  for the west valley release is SW, followed by W, SE, NE, and S. With the enhancement of the background wind field (changing from stable weather to the strong cold air process), the  $P$  for W and SW gradually increases, whereas the  $P$  for SE and NE gradually decreases. The particles released in the east valley have a significantly higher chance of being transported across the southern mountains accompanied by the conversion from stable weather to the strong cold air process. Previous studies have suggested that manually

changing the terrain is one of the methods to decrease air pollution in Lanzhou [13]. Identifying the transport channels is conducive to achieving this goal.

**Table 1.** Percentage of particles passing through the five typical transport channels under different circulation types and average states (units: %/km).

Weather	Typical Transport Channels									
	East Valley Release					West Valley Release				
	SW	W	S	SE	NE	SW	W	S	SE	NE
CT1	0.549	0.247	0.336	1.168	0.556	1.081	0.436	0.150	0.440	0.472
CT2	0.551	0.239	0.207	1.338	0.480	0.931	0.447	0.118	0.453	0.495
CT3	0.675	0.272	0.611	1.022	0.462	1.411	0.506	0.245	0.303	0.251
CT4	0.799	0.288	0.339	1.047	0.335	1.412	0.571	0.179	0.241	0.265
CT5	0.808	0.277	0.615	0.842	0.276	1.591	0.629	0.175	0.166	0.231
CT6	0.838	0.277	0.798	0.817	0.361	1.922	0.623	0.210	0.079	0.148
CT7	0.615	0.272	0.367	1.211	0.615	1.300	0.395	0.236	0.437	0.475
CT8	1.012	0.342	0.765	0.678	0.210	1.932	0.694	0.139	0.111	0.072
Mean	0.733	0.277	0.493	1.107	0.413	1.441	0.543	0.180	0.279	0.300

Figure 5 shows the percentage of particles moving out of the urban valley after 12 h of transport (hereafter referred to as PMO) and the ratio of particles moving back into the urban valley (hereafter referred to as PMB). The efficiency of transport to the outside of the valley is a key factor influencing the air quality in Lanzhou. After 12 h of transport, more than 80% of the particles moved out of the urban valley. Particles released from 5:00 BT to 13:00 BT were more easily transported out of the valley. The PMO then decreased gradually with a minimum at 22:00 BT and then increased rapidly. The PMO released in the west valley from 8:00 BT to 14:00 BT was higher than that released in the east valley. However, the PMO released in the west valley from 15:00 BT to 4:00 BT (next day) was lower than that released in the east valley. More than 98% of the particles moved out of the urban valley after 24 h of transport (figures not shown). The ratio of particles moving back into the valley is also an important factor influencing the air quality in Lanzhou. The PMB released in the east valley was higher than that released in the west valley. The maximum and minimum of the PMB released in the east valley occurred at 23:00 BT and 07:00 BT and at 19:00 BT and 11:00 BT for the west valley, respectively. To some extent, the high PMB released in the east valley counteracted the effect of the high PMO. This finding indicates that the air pollution over Lanzhou can be reduced to some extent by artificially controlling the emission time of pollutants, such as adjusting the working hours of the factory.

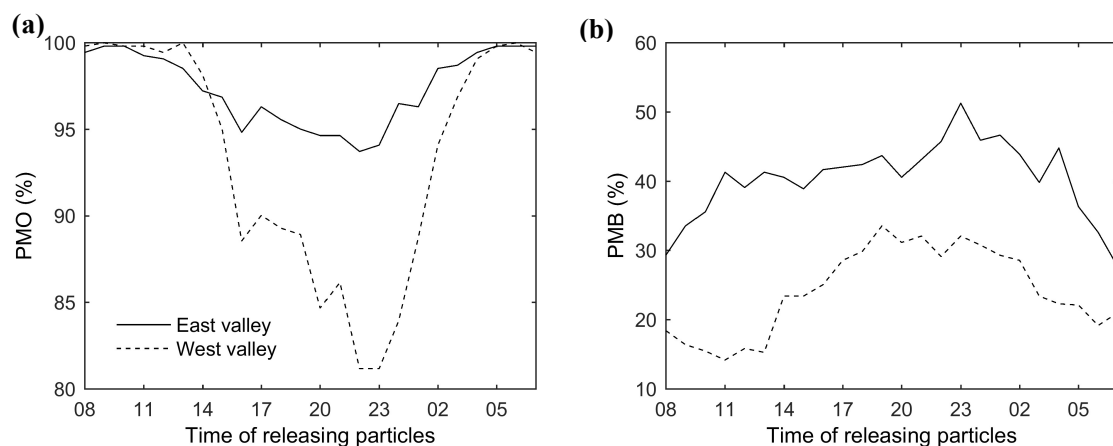


**Figure 5.** (a) Percentage of particles moving out of the urban valley after 12 h of transport (PMO) and (b) Ratio of particles moving back into the urban valley (PMB). The type of lines represents the location of released point.

#### 4. Conclusions

Lanzhou, a typical valley city in northwest China, has suffered serious air pollution. However, the pollutant transport pathways from local emissions to outside of the valley are still unclear. Using the WRF-FLEXPART model, the authors of this paper analyzed the transport characteristics over Lanzhou during six winters from 2002 to 2007.

Mountain–valley winds and the urban heat island effect are two important factors influencing local circulation over Lanzhou. The near-surface wind covering the Lanzhou valley is an easterly wind. The local wind field determines the pollutant transport trajectories to some extent. Five typical transport channels, namely, the southwest pathway, west pathway, south pathway, southeast pathway, and northeast pathway, were identified. In general, the largest percentage of particles in the east valley release passed through the southeast pathway, followed by the southwest, south, northeast, and west pathways. The largest percentage of particles in the west valley release passed through the southwest pathway, followed by the west, southeast, northeast, and south pathways. The synoptic-scale circulation type had a significant effect on the transport channels of pollutants released from urban Lanzhou. Compared with static weather, it was easier for pollutants to cross the south mountain during the strong cold air process. The percentage of particles moving out of the urban valley after 12 h of transport and the ratio of particles moving back into the urban valley displayed significant diurnal variability. This indicates that the air pollution over Lanzhou can be reduced to some extent by artificially controlling the emission time of pollutants.

The findings of this paper promote the understanding of air pollution characteristics and air pollution control over Lanzhou. More research, on topics such as the atmospheric environmental capacity and the transport characteristics of different seasons, should be carried out in the future.

**Author Contributions:** This research work was mainly conducted by J.H. He also compiled the manuscript. Y.Y. and S.G. were the principle investigators on the project. S.L., S.Z., and C.Z. contributed with results analysis and the revision of the manuscript.

**Funding:** This work was supported by the National Natural Science Foundation of China (Nos. 41705080 and 91544232), the CAMS Basis Research Project (No. 2017Y001), the National Science and Technology Infrastructure Programme (No. 2014BAC16B03), and the CMA Innovation Team for Haze–Fog Observation and Forecasts.

**Conflicts of Interest:** The authors declare no conflict of interest.

#### References

1. He, J.; Gong, S.; Yu, Y.; Yu, L.; Wu, L.; Mao, H.; Song, C.; Zhao, S.; Liu, H.; Li, X.; et al. Air pollution characteristics and their relation to meteorological conditions during 2014–2015 in major Chinese cities. *Environ. Pollut.* **2017**, *223*, 484–496. [[CrossRef](#)] [[PubMed](#)]
2. Song, C.; He, J.; Wu, L.; Jin, T.; Chen, X.; Li, R.; Ren, P.; Zhang, L.; Mao, H. Health burden attributable to ambient PM<sub>2.5</sub> in China. *Environ. Pollut.* **2017**, *223*, 575–586. [[CrossRef](#)] [[PubMed](#)]
3. Avnery, S.; Mauzerall, D.L.; Liu, J.; Horowitz, L.W. Global crop yield reductions due to surface ozone exposure: 1. Year 2000 crop production losses and economic damage. *Atmos. Environ.* **2011**, *45*, 2284–2296. [[CrossRef](#)]
4. Chen, Y.; Zhao, C.S.; Zhang, Q.; Deng, Z.Z.; Huang, M.Y.; Ma, X.C. Aircraft study of Mountain Chimney Effect of Beijing, China. *J. Geophys. Res.* **2009**, *114*, D08306. [[CrossRef](#)]
5. Crippa, M.; Canonaco, F.; Slowik, J.G.; El Haddad, I.; DeCarlo, P.F.; Mohr, C.; Heringa, M.F.; Chirico, R.; Marchand, N.; Temime-Roussel, B.; et al. Primary and secondary organic aerosol origin by combined gas-particle phase source apportionment. *Atmos. Chem. Phys.* **2013**, *13*, 8411–8426. [[CrossRef](#)]
6. He, J.; Wu, L.; Mao, H.; Li, R. Impacts of meteorological conditions on air quality in urban Langfang, Hebei Province. *Res. Environ. Sci.* **2016**, *29*, 791–799. (In Chinese)
7. Vivanco, M.; Theobald, M.; García-Gómez, H.; Garrido, J.; Prank, M.; Aas, W.; Adani, M.; Alyuz, U.; Andersson, C.; Bellasio, R.; et al. Modeled deposition of nitrogen and sulfur in Europe estimated by 14 air quality model systems: evaluation, effects of changes in emissions and implications for habitat protection. *Atmos. Chem. Phys.* **2018**, *18*, 10199–10218. [[CrossRef](#)]

8. Saikawa, E.; Kim, H.; Zhong, M.; Avramov, A.; Zhao, Y.; Janssens-Maenhout, G.; Kurokawa, J.; Klimont, Z.; Wagner, F.; Naik, V.; et al. Comparison of emissions inventories of anthropogenic air pollutants and greenhouse gases in China. *Atmos. Chem. Phys.* **2017**, *17*, 6393–6421. [[CrossRef](#)]
9. Ning, J.; Gao, J.; Zheng, J.; Jia, N.; Xian, Z.; Li, X.; Mao, Y.; Sheng, L.; Song, Y.; Zeng, Y.; et al. *China Statistical Yearbook*; China Statistics Press: Beijing, China, 2017. Available online: <http://www.stats.gov.cn/tjsj/ndsj/2017/indexch.htm> (accessed on 1 August 2018).
10. Shi, C.; Yuan, R.; Wu, B.; Meng, Y.; Zhang, H.; Zhang, H.Q.; Gong, Z. Meteorological conditions conducive to PM<sub>2.5</sub> pollution in winter 2016/2017 in the Western Yangtze River Delta, China. *Sci. Total Environ.* **2018**, *642*, 1221–1232. [[CrossRef](#)] [[PubMed](#)]
11. He, J.; Yu, Y.; Chen, J.; Liu, N.; Zhao, S. Simulation study of the influence of vegetation fraction on meteorological condition in Lanzhou using WRF model. *Plateau Meteorol.* **2012**, *31*, 1611–1621. (In Chinese)
12. Wang, S.; Feng, X.; Zeng, X.; Ma, Y.; Shang, K. A study on variations of concentrations of particulate matter with different sizes in Lanzhou, China. *Atmos. Environ.* **2009**, *43*, 2823–2828. [[CrossRef](#)]
13. Hu, Y.; Zhang, Q. Atmosphere pollution mechanism along with prevention and cure countermeasure of the Lanzhou hollow basin. *China Environ. Sci.* **1999**, *19*, 119–122. (In Chinese)
14. He, J.; Yu, Y.; Xie, Y.; Mao, H.; Wu, L.; Liu, N.; Zhao, S. Numerical model-based artificial neural network model and its application for quantifying impact factors of urban air quality. *Water Air Soil Poll.* **2016**, *227*, 235. [[CrossRef](#)]
15. Zhang, Q.; Li, H. A study of the relationship between air pollutants and inversion in the PBL over the city of Lanzhou. *Adv. Atmos. Sci.* **2011**, *28*, 879–886. [[CrossRef](#)]
16. An, X.; Zuo, H.; Chen, L. Atmospheric environmental capacity of SO<sub>2</sub> in winter over Lanzhou in China: A case study. *Adv. Atmos. Sci.* **2007**, *24*, 688–699. [[CrossRef](#)]
17. Yu, Y.; He, J.; Zhao, S.; Liu, N.; Chen, J.; Mao, H.; Wu, L. Numerical simulation of the impact of reforestation on winter meteorology and environment in a semi-arid urban valley, Northwestern China. *Sci. Total Environ.* **2016**, *569–570*, 404–415. [[CrossRef](#)] [[PubMed](#)]
18. Liu, N.; Yu, Y.; He, J.; Zhao, S. Integrated modeling of urban-scale pollutant transport: Application in a semi-arid urban valley, Northwestern China. *Atmos. Pollut. Res.* **2013**, *4*, 306–314. [[CrossRef](#)]
19. Skamarock, W.; Klemp, J. A time-split nonhydrostatic atmospheric model for weather research and forecasting applications. *J. Comput. Phys.* **2008**, *227*, 3465–3485. [[CrossRef](#)]
20. Hong, S.; Lim, J. The WRF Single-Moment 6-Class Microphysics Scheme. *Korean Meteor. Soc.* **2006**, *42*, 129–151.
21. Kain, J. The Kain-Fritsch convective parameterization: An update. *J. Appl. Meteorol. Clim.* **2004**, *43*, 170–181. [[CrossRef](#)]
22. Mlawer, E.; Taubman, S.; Brown, P.; Iacono, M.; Clough, S. Radiative transfer for inhomogeneous atmosphere: RRTM, a validated correlated-k model for longwave. *J. Geophys. Res.* **1997**, *102*, 16663–16682. [[CrossRef](#)]
23. Dudhia, J. Numerical study of convection observed during the winter monsoon experiment using a mesoscale two-dimensional model. *J. Atmos. Sci.* **1989**, *46*, 3077–3107. [[CrossRef](#)]
24. Hong, S.; Noh, Y.; Dudhia, J. A new vertical diffusion package with an explicit treatment of entrainment processes. *Mon. Weather Rev.* **2006**, *134*, 2318–2341. [[CrossRef](#)]
25. Chen, F.; Dudhia, J. Coupling an advanced land surface-hydrology model with the Penn State-NCAR MM5 modeling system. Part I: model implementation and sensitivity. *Mon. Weather Rev.* **2001**, *129*, 569–585. [[CrossRef](#)]
26. Lo, J.; Yang, Z.; Pielke, R. Assessment of three dynamical climate downscaling methods using the weather research and forecasting (WRF) model. *J. Geophys. Res.* **2008**, *113*, D09112. [[CrossRef](#)]
27. Heikkilä, U.; Sandvik, A.; Sorteberg, A. Dynamical downscaling of ERA-40 in complex terrain using the WRF regional climate model. *Clim. Dyn.* **2011**, *37*, 1551–1564. [[CrossRef](#)]
28. Brioude, J.; Arnold, D.; Stohl, A.; Cassiani, M.; Morton, D.; Seibert, P.; Angevine, W.; Evan, S.; Dingwell, A.; Fast, J.; et al. The Lagrangian particle dispersion model FLEXPART-WRF version 3.1. *Geosci. Model Dev.* **2013**, *6*, 1889–1904. [[CrossRef](#)]
29. Brioude, J.; Angevine, W.; McKeen, S.; Hsie, E. Numerical uncertainty at mesoscale in a Lagrangian model in complex terrain. *Geosci. Model Dev.* **2012**, *5*, 1127–1136. [[CrossRef](#)]

